4th Workshop on Measurement Technique for
Stationary and Transient Two-Phase Flows
Rossendorf, Germany, November 16-17, 2000

ULTRASONIC DOPPLER METHOD FOR BUBBLY FLOW MEASUREMENT

Masanori Aritomi, Hiroshige Kikura and Yumiko Suzuki

Research Laboratory for Nuclear Reactors, Tokyo Institute of Technology
2-12-1 Ohokayama, Meguro-ku, Tokyo 152-8550, Japan

ABSTRACT

The Ultrasonic Velocity Profile technique has been developed to measure multi-dimensional flow characteristics in bubbly flows with the void fraction smaller than 7%. This measurement system can measure instantaneous mixture velocity profiles along a measuring line. By analyzing statistically the measured data, velocity profiles of both phases, the void fraction profile, turbulence intensity of the liquid phase in a channel and flow structure of the liquid phase surrounding a bubble can be obtained. The flow structure around bubbles was proposed to be divided into three regions: viscous sublayer, buffer region, and turbulence region.

Keywords: Bubbly flow measurement, Velocity profiles, Ultrasonic Doppler measurement

1. INTRODUCTION

The flow structure surrounding bubbles is one of the interesting topics in the field of two-phase bubbly flow. A great number of experimental studies have been carried out to understand the fundamental mechanism of two-phase flows. The quick closing valves is one of the most simple and early-developed methods to measure the average void fraction of steady and uniform two-phase flow [1]. To measure local void fraction, probe techniques and radiation techniques have been used for a long time [2] and [3]. In recent years, a laser Doppler anemometer has been applied to the bubbly flow measurement as a strong device to investigate the flow structure in detail, such as local void fraction profile, liquid velocity and its fluctuation [4] and [5]. Flow visualization techniques have also been used commonly in order to understand bubble deformation and coalescence phenomena [6] and [7]. These methods have made a great contribution in clarifying the flow structure of the bubbly two-phase flow. However, there still does not exist a measurement technique which can easily measure the velocity profile around a gas-liquid interface, even though it is necessary to clarify the flow structure around the bubble surface in order to understand the microscopic mechanism of bubbly flows.

The authors attempt to apply UVP method to measure multi-dimensional flow characteristics in bubbly flows with void fraction less than 7%. The ultrasonic pulse is reflected on both micro-particles in liquid phase and gas-liquid interfaces, so that instantaneous mixture velocity profile along the measuring line can be measured. By

treating statistically the measured instantaneous mixture velocity profile, a probability density function profile of the mixture velocities can be obtained. From the results, velocity profiles of both phases, the void fraction profile, turbulence intensity of the liquid phase can be obtained in a channel. Since velocity information of both phases is included in the measured instantaneous mixture velocity profile, the phase discrimination of the measured instantaneous mixture velocity profile is one of the important processes in order to study the flow structure of liquid phase surrounding bubbles. From the measured instantaneous velocity profiles, the position of the bubble surface was decided and the data was rearranged according to the distance from the bubble surface.

In this paper, a measurement system using the UVP monitor is proposed and its measurement principle is explained first. Furthermore, the proposed measurement system is applied to bubbly flows in a vertical rectangular channel to verify its capability. Finally, improvement of the proposed measurement system is discussed as our future work.

2. MEASUREMENT METHOD OF ULTRASONIC VELOCITY PROFILE MONITOR

2.1 Experimental Setup

Figure 1 shows the schematic diagram of the experimental apparatus. It consisted of a water circulation system, an air supply system, a test section which is a rectangular channel made of Plexiglas and a measurement system of Ultrasonic Velocity Profile (UVP) monitor. Working fluids were air and tap water. Micro particles of nylon powder were mixed in the water as reflector of ultrasonic pulses. The average diameter of the powder was about 40 μm, and the specific density was 1.02.

In the measurement of counter-current flows, water was fed from the upper tank into the test section. Water flow rate was controlled by a needle valve and it was measured by an orifice flowmeter, both of which were located at the bottom part of the apparatus. Air was injected into water through five needles (inner diameter: 0.17 mm) at the air-water mixing section, which were also located at the lower end of the test section. The air flow rate was regulated by a float flow meter and an air control valve. In the measurement of co-current flows, water flowed upward into the test section from the lower entrance of the test section. Air was injected from the same air-injection needles as those of the counter-current flows. During an experiment, water temperature was kept between 19 and 21 degrees using a subcooling system. Also in parallel to the measurement by the UVP, the pressure drop was measured between pressure taps installed on the sidewall to get average void fraction. All experiments were carried out under the atmospheric pressure.

Figure 2 shows the test section located between the upper tank and the air-water mixer. The test section was a vertical rectangular channel made of Plexiglas measuring 10 mm $\times$ 100 mm $\times$ 1700 mm. An ultrasonic transducer was set on the outer surface with a contact angle of 45 degrees toward the liquid main flow direction. Gap between the transducer and the wall was filled with ultrasonic jelly to

prevent the reflection of ultrasonic pulses on the wall. Under each experimental condition, measurement was carried out and 9,216 velocity profiles were obtained along the measuring line. The experimental conditions are tabulated in Table 1. Also, the UVP configurations used in this study are summarized in Table 2.

An outline of video camera equipment is shown in Fig.3. It consists of a digital video camera, alight source and a translucent sheet to unify the luminance brightness. The speed, diaphragm and gain of the video camera can be manually regulated and a speed of 60 flames per second can be obtained. After videotaping, the video digital data were recorded in a personal computer through an image converter. The picture elements were 720×480 dots, the color was monotone, and the brightness resolution was 1/256. Figure 4 is an example of the photos of the counter-current flow. In Fig. 5, the relationship between the average void fraction in the channel and average bubble diameter is shown.

2.2 Measurement Principle

The working principle of the UVP is to use the information contained in the echo of ultrasonic pulses reflected by micro particles suspended in the fluid. Since the detailed information of its measurement principle has been reported by Takeda [8], [9], only a simple explanation is made here.

The position information, x, is obtained from the time lapsed, τ, from the emission to the reception of the echo:

$$x = \frac{c\tau}{2} \tag{1}$$

where c is a speed of sound in the fluid. The instantaneous local velocity, $u_{UVP}(x)$, is a component along the ultrasonic beam direction and is derived from the instantaneous Doppler shift frequency, f_D, in the echo:

$$u_{UVP} = \frac{cf_D}{2f} \tag{2}$$

where f is the basic ultrasonic frequency. The velocity resolution is given by

$$\delta u_{UVP} = \frac{u_{UVPmax}}{128} \tag{3}$$

The measured velocity profile is expressed by a location number, i, a profile number, j, and a velocity value, k.

$$k = u[i, j] \tag{4}$$

The position, $y(i)$, is determined from the wall location, i_1 and i_2 as

$$y(i) = \frac{i - i_1}{i_2 - i_1} W \tag{5}$$

where W is the width of the channel, 10mm.

The measured velocity, which is a component along the ultrasonic beam direction, u_{UVP}, is determined by

$$u_{UVP} = k\Delta u \tag{6}$$

where Δu is the conversion factor from Doppler unit to velocity. The velocity in the flow direction, u, is then given by

$$u = \frac{u_{UVP}}{\cos\theta} \tag{7}$$

where θ is the angle of the transducer with respect to the flow direction. The measurement error of velocity is estimated as ±5%.

2.3 Data Processing Method

Since the speed of sound of longitudinal waves is the most fundamental parameter for this method, it is incorrect to treat a two-phase medium as a homogeneous single phase medium because sound waves experience multiple reflection at bubbles. Since the ultrasonic pulse diameter using in this work is 5mm, which is larger than bubble diameter of about 3mm, the ultrasonic pulse and its reflection can potentially traverse straight on while creating a blind zone behind the bubble as shown in Fig.6. Typical patterns of instantaneous velocity profiles are shown in Fig.7 (a), (b) and (c): (a) is the case where there is no bubble in the measurement path, (b) is the case where a single bubble exists and (c) is the case where two bubbles exist. In case of Fig.7 (c), we cannot distinguish whether two bubbles exist in the measurement volume or if there are multiple reflection between bubbles as shown Fig.8 (a) and (b). Since a velocity profile like that shown in Fig.7(c) is rarely encountered under the present experimental conditions, it is omitted while data processing in this study. It is however, possible to obtain velocity profiles of the liquid phase, even at high void fraction, until a bubble approaches the transducer. The authors thus attempted to derive information from each individual profiles by analyzing their shapes.

Although the spatial resolution of the UVP measurement is not particularly fine because the ultrasonic beam diameter is 5mm, the nearly instantaneous water velocity profile near a bubble can be measured by the UVP measurement as shown in Figs. 7(b) and 7(c). If many velocity profiles are obtained and treated statistically, the flow characteristics near a bubble may be deduced.

2.3.1 Angle of the Ultrasonic Transducer

Since the velocity information is derived from the Doppler shift frequency, no data must exist at the wall. The diameter of the ultrasonic pulse beam is 5mm and the UVP transducer must be inclined with respect to the wall in order to measure velocities in the flow direction. Figure 9 (a), (b) and (c) show typical results of frequency of data existence in reference to the transducer angle at the wall. In single phase water flow, it can be seen from Fig. 9(c) that with the setting angle at 75ß, we have the most suitable angle in terms of the frequency of data existence. However, it is seen from Figs.9 (a) (b) and (c) that a transducer angle of 45ß is best in bubbly

flows to prevent multiple reflection. The ultrasonic pulse is perfectly reflected at the channel wall and can not be transmitted into the fluid. Therefore, a transducer angle of 45ß is adopted in this work.

2.3.2 Velocity and Void Fraction Profile in the Channel

The probability of data existence was examined along ultrasonic beam direction. It can be seen from Fig. 9(a) that the wall position is identical to the location where the probability of data existence is 50% in single phase liquid flow. The measurement error of the wall position is estimated as ±0.1mm and the measurement error of the location is estimated as ±0.6mm. Since the diameter of an ultrasonic pulse is 5mm, its measurement cross section is a circular disk in the main region of flow and the echo can be completely measured in the form of the circular cross section. On the other hand, the measurement cross section can not be circular near the wall region, so that the statistical average position of the measurement cross section is not the center of ultrasonic pulse. Assuming that the statistical average position of the measurement cross section divides the measuring cross section into two equal cross sections, the statistical average position is revised. Thus, the measuring cross sectional area less than 50% of the whole ultrasonic beam is omitted.

The probability of data existence, $P_1(y)$, is defined by

$$P_1(i) = \sum_{j=1}^{N} f_1(i,j) \Big/ N \,, \tag{8}$$

$$f_1(i,j) = 1 \quad \text{for} \quad V[i,j] \neq 0,$$
$$= 0 \quad \text{for} \quad V[i,j] = 0,$$

where N is the number of total profiles. A profile of the probability of data existence, $P_s(y)$, is obtained by converting the location number, i, into a real position, y.

Let us consider a velocity probability function:

$$P_2(i,k) = \sum_{J=1}^{N} f_2(i,j) \Big/ \sum_{J=1}^{N} f_1(i,j) \tag{9}$$

$$f_2(i,j) = 1 \quad \text{for} \quad V[i,j] = k,$$
$$= 0 \quad \text{for} \quad V[i,j] \neq k.$$

A probability density function, $P_u(y,u)$, is obtained by normalizing $P_2(i,j)$ and by converting the location number, i, into a real position.

A probability density function includes the velocity information. It is assumed that each probability density function of a given phase can be expressed by a normal distribution, as follows:

$$N[\bar{u},\sigma^2](u) = \frac{1}{\sqrt{2\pi\sigma^2}} exp\left[-\frac{(u-\bar{u})^2}{2\sigma^2} \right] \tag{10}$$

The probability density function of the mixture velocity is given by

$$P_v(y,u) = \varepsilon(y) N[\overline{u_G}(y), \sigma_G^2(y)](u) + (1-\varepsilon(y)) N[\overline{u_L}(y), \sigma_L^2(y)](u) \tag{11}$$

where σ_G and σ_L are average velocities and standard deviations of both phases respectively, and ε is the probability of bubble existence. These five variables, σ_G, σ_L and ε, are calculated numerically by the least-squares method.

Figure 10 compares a probability density function of mixture velocities calculated by the above-mentioned procedure with experimental results. In this figure, open circles indicate the results measured by the UVP and the line represents the calculated result.

Since the ultrasonic pulse is reflected at the interface as long as a bubble exists, the bubble velocity can always be detected as an interfacial velocity. On the other hand, the ultrasonic wave is not reflected in water where a micro-particle does not exist. As a result, the water velocity is not always measured in the profile. Therefore, it is necessary to revise the probability of bubble existence as follows:

$$\kappa(y) = P_s(y)\varepsilon(y) \tag{12}$$

where $\varepsilon(y)$ is called the probability of bubble data existence in this work.

The probability of bubble data existence means that a bubble exists in the path of the ultrasonic pulse when the pulse is emitted, and is related to the void fraction. The bubble size, its position and its configuration cannot be known directly from UVP measurements. Assuming that the bubble size and configuration are at random and that they are statistically uniform across the channel, the conversion factor, which relates the probability of bubble data existence to the void fraction, can be obtained. The following procedure was developed to establish the conversion factor.

The average volumetric flux of the bubble $\langle j_G \rangle$ is

$$\langle j_G \rangle = \frac{\int_A j_G dA}{A} = \frac{\int_A \alpha u_G dA}{A} \tag{13}$$

where j_G is the local volumetric flux of the bubble and A is the cross sectional area of the channel. Assuming that the local void fraction is proportional to the local probability of bubble data existence and that the proportionality constant (the conversion factor), k, is uniform in the channel since it is dependent on bubble size and configuration, the following equation can be obtained:

$$\langle j_G \rangle = k \frac{\int_A \kappa u_G dA}{A} \tag{14}$$

The average void fraction is expressed by

$$\langle \alpha \rangle = \frac{k \int_A \kappa dA}{A} \tag{15}$$

If the air flow rate is known, we can transform Eq.(14) to

$$k = \frac{\langle j_G \rangle A}{\int_A \kappa u_G dA} = \frac{\langle j_G \rangle}{\langle \kappa u_G \rangle} \tag{16}$$

Then, the local void fraction, $\alpha(y)$, is simply given by

$$\alpha(y) = k\kappa(y). \tag{17}$$

The average void fraction, $\langle\alpha\rangle$, is also represented by

$$\langle\alpha\rangle = k\langle\kappa\rangle. \tag{18}$$

2.3.3 Velocity Profile around Bubbles

When the UVP is used for the measurement of bubbly flow, ultrasonic pulses are reflected either on a gas-liquid interface or micro particles suspended in the liquid, and then the velocity profiles in the channel is obtained. Therefore a measured velocity profile contains not only liquid phase velocity information but also the bubble-rising velocity information, which is obtained from pulses reflected on the bubble's surface. In the measuring of bubbly flow, an instantaneous velocity profile has a typical peak if a bubble crosses the measuring line. The maximum velocity in the instantaneous velocity profile including bubble is much larger than the one excluding bubbles. By introducing an appropriate threshold velocity, the recorded instantaneous velocity profile can be divided into two groups, that is, profiles either including bubbles or not.

Figure 11 shows a flow chart of data processing. The first step in the determination of the threshold velocity is to obtain the probability density function of all the measured 27,648 instantaneous velocities at each measuring position. This is called "PDF_{all}" (Fig. 12(a)). Velocity information of both phases is mixed up in this PDF_{all}. When the void fraction is very low, PDF_{all} have usually two peaks; one represents the liquid velocity and the other stands for the velocity concerning the gas-rising velocity. However in some experimental conditions, only one peak is seen, which corresponds to the liquid velocity. Since the PDF_{all} also contains liquid velocity accelerated by the gas phase, the PDF_{all} monotonously decreases from the peak of liquid phase toward the velocity of gas phase. The mixture of these liquid velocities makes the phase discrimination difficult.

As the second step, liquid main flow velocity is separated from PDF_{all}. The peak velocity of the liquid phase in the PDF_{all} is chosen as the representative velocity of the liquid phase, u_{Lm}. By assuming that the ideal shape of PDF for the liquid main flow velocity is symmetrical because of the symmetric nature of the random error, PDF of the liquid phase can be estimated by turning up the left-hand side of the PDF for the liquid phase at the u_{Lm}. From the obtained PDF, called the ideal PDF for the liquid main flow, standard deviation σ_L is calculated. By taking into account the fluctuation of liquid velocity, the threshold velocity for separation of the liquid main flow, $u_{temp,}$ is obtained as $u_{temp} = u_{Lm} + 2\sigma_L$

At this time another PDF, PDF_{max}, is defined representing the gas velocity (Fig. 12(b)). PDF_{max} at each measuring position is obtained by collecting only the largest velocity in each instantaneous velocity profile. Most of the velocity information included in PDF_{max} is either the bubble's velocity or the maximum velocity of the liquid phase in the case not including bubbles. Therefore if the liquid phase velocity

is separated from PDF_{max}, PDF corresponding to the bubble's velocity can be obtained. For the separation of liquid velocities, u_{temp} at the same measuring point is used and data smaller than u_{temp} is eliminated from the PDF_{max}.

From the remaining PDF, the average velocity u_{Gm} and the standard deviation σ_G is calculated. By using these values, finally the threshold velocity for the phase separation u_{thresh} is obtained as $u_{thresh} = u_{Gm} - 2\sigma_G$ (Fig. 12(b)). The calculation of the u_{thresh} is made at each measuring point in the channel according to the above procedure and the threshold velocity profile $u_{thresh}(x)$ is obtained as a result. Using this threshold velocity profile, phase discrimination is made for each instantaneous velocity profile.

The measured instantaneous velocity profile including only velocities lower than u_{thresh} means the liquid velocity one affected by bubble rising motion and is classified into Group A. By averaging velocities in Group A, the time-averaged velocity profile of liquid main flow can be obtained. On the other hand, the measured instantaneous velocity profile whose maximum velocity higher than u_{thresh} has bubble motion information and is classified into Group B. In Group B, the relative coordinate is adopted and its origin is set on the bubble surface for the selected instantaneous velocity profiles. In order to examine the flow structure surrounding a bubble, the selected velocity profiles are statistically treated by converting their data as a function of the distance from a bubble surface, and thus the probability density function of liquid velocity fluctuation is calculated at each distance from a bubble surface.

After splitting all instantaneous velocity profiles into two groups, probability density functions of instantaneous velocities are calculated at every measuring point in the channel. From the obtained shape of the probability density function, statistical moments were calculated for the liquid phase velocity as follows:

$$M = \int_{-\infty}^{\infty} (u - c)^n P_u(x) du \tag{19}$$

where u means a measured velocity, $P_u(x)$ a probability density and

$c = 0$ for the first order moment,
$= U$ for higher order moments.

where U is the first order moment that means the average velocity. The second order moment means the standard deviation of velocity fluctuation, σ_2, called variance, the third dimensionless one, M_3/σ_3, is called the skewness and the fourth dimensionless one, M_4/σ_4, is the kurtosis.

3. EXPERIMENTAL RESULTS

3.1 Velocity Profile in the Channel

The developed measurement system was applied to bubbly countercurrent flows in a vertical rectangular channel. Figure 13(a) and (b) shows typical measurements of velocity profiles in both phases, u_G and u_L, and a probability profile of bubble data

existence, $\kappa(y)$. The velocities of both phases are not zero at the wall because the ultrasonic pulse is emitted at an angle with respect to the channel wall and its beam diameter is 5mm, the combined effect of which induces an error in the velocity measurements near the wall. However, this uncertainty is not a feature of two-phase flow measurement, but also appears for the velocity profiles measured in a single-phase flow by the UVP.

3.2 Void Fraction Profile

Let us consider another procedure in order to estimate the conversion factor between the probability of bubble data existence and the void fraction using the average void fraction measured by the image data processing unit. Assuming that an entire bubble exists in the path of the ultrasound beam when the pulse is emitted, the measurement volume, V_1, is expressed by

$$V_1 = \frac{1}{4}\pi D_u^2 L \tag{20}$$

where D_u is the ultrasound pulse diameter and L is the UVP measurement length. The bubble volume is

$$V_b = \frac{1}{6}\pi D_b^3 \tag{21}$$

where D_b is the average bubble diameter. The conversion factor, k_1, can be given by

$$k_1 = \frac{V_b}{V_1} = \frac{2D_b^3}{3D_u^2 L} \tag{22}$$

If a vertical portion of the bubble's surface encounters the path of the pulse, the ultrasonic transducer may receive the reflection wave of this pulse. Hence, we consider the case where a half of a bubble exists in the pulse path. In this case, the UVP measurement volume, V_2, can be expressed by

$$V_2 = \frac{1}{4}\pi\left(D_u + D_b\right)^2 L \tag{23}$$

The conversion factor k_2 is

$$k_2 = \frac{V_b}{V_2} = \frac{2D_b^3}{3\left(D_u + D_b\right)^2 L} \tag{24}$$

The conversion factors obtained from experiments are shown in Fig.14 in reference to average bubble diameters. k_1 and k_2 are shown in the figure. It is seen from the figure that k_v, is located in the region of $k_2<k_v<k_1$. Although the conversion factor cannot be evaluated exactly because of a wide range between k_1 and k_2, it is apparent that the factor depends on the average bubble diameter. Since the bubble is not spherical, the factor may also be influenced by the bubble shape. However, its empirical correlation can be established by analyzing numerous data. Moreover, it seems that the conversion factor can be established from the UVP data if each data profile is analyzed in detail and for instance, pattern recognition of the echo signal is established. These are topics of future studies.

The conversion factor can also be calculated by the average void fraction obtained from the hydrostatic head measurement and by the average probability of bubble data existence. Figure 15 shows a typical void fraction profile converted from the probability profile of bubble data existence in this way. As mentioned above, the average void fraction in the flow cross section is estimated as ±5%. Regarding the local void fraction, although the error introduced by the assuming uniformity in the conversion factor between the local void fraction and the local probability of bubble data existence in the cross section of the flow cannot be evaluated exactly, the error in the local void fraction may be estimated as ±10%.

3.3 Turbulent Intensity Profile

In general, turbulence intensity in a bubbly flow is larger than that in liquid single phase flow because bubbles agitate the flow. In this work, turbulence intensity is defined in terms of the standard deviation of water velocity fluctuation in the continuous phase, σ_L. The standard deviation profile in the channel can be calculated from the equation of the probability density function of mixture velocity defined by Eq.(11). Typical results from single-phase water flow and bubbly countercurrent flow are shown in Fig.16. Since the local velocities were not measured at a point but over an area because of the size of the ultrasonic beam diameter (5mm), the absolute value of the standard deviation in the water phase is not significant. Hence, the standard deviation ratio of a bubbly countercurrent flow to a single phase water flow is selected as the two-phase multiplier of turbulence intensity, $\sigma_{LTPF} / \sigma_{LSPF}$.

3.4 Velocity Profile around Bubbles

Figure 17 shows typical profiles of the probability density function of relative velocity in reference to the distance from a bubble surface. In the figure, x=0 means a bubble surface and x=1 is the position 0.74mm away from the bubble surface.

The probability density function near a bubble surface (x=0-1) has a one peak which means the rising velocity of the bubble motion. In the region of x=2-10, two peaks appear, which correspond to the bubble surface velocity and main flow. The peak corresponding to the bubble surface velocity becomes lower and the other peak does larger with going way from the bubble. In the region far from the bubble (x=11-14), the probability density function has one peak again which is the main flow.

Figure 18 (a) shows a typical a velocity profile normalized by the average bubble surface and liquid main velocities. Moreover, profiles of typical valiance, skewness and kurtosis are shown in Fig.18 (b), (c) and (d). It can be seen from different gradients shown in these figures that the liquid flow structure can be classified into three regions; (1) viscous sublayer region near a bubble where the liquid flow is greatly influenced only by the bubble motion, (2) turbulence region far from a bubble where it is not affected by the bubble motion and (3) buffer region located between viscous sublayer and turbulence region where it is influenced by the bubble motion and the main flow.

Some velocity profiles of Group B have the second peak between the position the maximum velocity and the channel wall as shown in Fig.19. The second peak velocity means the effect of a bubble flowing near the measurement volume. For the purpose to investigate the effect of another bubble motion on the liquid flow structure surrounding bubbles, the measured instantaneous velocity profiles in Group B are classified into two groups: the profiles having two peaks (Group B1) and those having only one peak (Group B2). Figure 20 (a) shows velocity fields surrounding bubbles which belongs to Group B1 and is affected by the wake of another bubble. In contrast with this, velocity fields surrounding bubbles in Group B2, which are not influenced by the wake of another bubble, are shown in Fig.20 (b).

4. FUTURE WORKS

The proposed measurement system has never developed perfectly and some improvements remain as our future works. Void fraction profile cannot be measured directly and its measurement accuracy has never exactly understood. In addition, the conversion factor, *k*, cannot be evaluated analytically. Hence, it will be attempted to apply the electrode-mesh tomography method [10] together with the UVP monitor in order to measure void fraction profiles and clarify the measurement accuracy of the UVP monitor for void fraction profiles.

Since the ultrasonic pulse diameter of 5mm is too large to measure liquid flow structure surrounding bubbles as compared with the bubble diameter of 2 to 5mm, the liquid flow structure cannot be quantitatively clarified from the measured data. It will be, therefore, attempted that UVP transducer having the narrower measurement volume should be developed and be applied to measure the liquid flow structure surrounding bubbles.

5. CONCLUSIONS

A measurement system incorporating an UVP monitor has been developed and proposed for use in measuring multi-dimensional bubbly flow characteristics. The system has been applied to bubbly counter-current and co-current flows with void fraction less than 7% in a vertical rectangular channel to assess its capability.

(1) The proposed system can measure instantaneous mixture velocity profiles in the channel.
(2) By treating statistically the measured instantaneous mixture velocity profiles, the velocity profiles of both phases, the void fraction profile and turbulence intensity of the liquid phase in the channel can be obtained.
(3) The phase discrimination method of the measured instantaneous mixture velocity profile was proposed using the probability density function of the mixed velocities. The position of the bubble surface was decided and the data was rearranged according to the distance from the bubble surface. From the results, it can be seen that the liquid velocity field surrounding bubbles can be classified into the following three region; viscous sublayer, buffer region and turbulence region.

(4) In laminar sublayer, the liquid velocity profile has a large gradient, and is greatly affected by the bubble motion but hardly affected by the liquid main flow.
(5) The buffer region plays a role as a transition zone between the laminar sublayer and the main flow region. The motion of both phases influences the flow structure in this region.
(6) The main flow region is far away from bubbles, so that bubble motion does not affect the continuous liquid phase.

REFERENCE

[1] Liu, T.J., Int. Journal of Multiphase Flow, 219-1 (1993), 99.
[2] Serizawa, A., Kataoka, I., and Michiyoshi, I., Int. Journal of Multiphase Flow, 2 (1975), 235.
[3] Herringe, R.A., and Davis, M.R., Journal of Fluid Mechanics, 73 (1976), 97.
[4] Martin, W.W. et al., Int. Journal of Multiphase Flow, 7 (1981) 439.
[5] Monji, H., and Matsui, G., Two-Phase Flow Modelling and Experimentation 1995, (1995), 367.
[6] Katz, J., and Meneveau, C., Int. Journal of Multiphase Flow, 22-2 (1996), 239.
[7] Tokuhiro, A., et al., Int. Journal of Multiphase Flow, 24 (1998), 1383.
[8] Takeda, Y., Development of Ultrasound Velocity Profile Monitor, Nucl. Engrg. Des., 126 (1990) 277.
[9] Takeda, Y., Velocity Profile Measurement by Ultrasonic Doppler Method, Experimental Thermal and Fluid Science, 10 (1995) 444.
[10] Richter, S. and Aritomi, M., A New Electrode-Mesh Tomograph for Advanced Studies on Bubbly Flow Characteristics, Rossendorf (2000.11) to be published.

Table 1 Experimental condition

System pressure	Atmospheric pressure
Water superficial velocity (co-current flow)	0.12 - 0.18 (m/s)
Water superficial velocity (counter-current flow)	-0.06 - -0.12 (m/s)
Air superficial velocity (co-current flow)	0.00235 - 0.00384 (m/s)
Air superficial velocity (counter-current flow)	0.00195 - 0.00418 (m/s)

Table 2 Specification of the UVP (X-1)

Basic ultrasonic frequency	4 (MHz)
Maximum measurable depth	91- 758 (mm)
Velocity resolution	5.6 - 0.75 (mm/s)
Time resolution	16.4 - 131 (msec)
Spatial resolution in water	0.74 (mm)
Measurement points	128
Number of profiles	1024×9

1. Overflow tank
2. Pressure tap
3. Test section
4. Pressure sensor
5. Oscilloscope
6. UVP monitor
7. US transducer
8. Compressor
9. Storage tank
10. Air water mixer
11. Flowmeter
12. Orifice flowmeter
13. PC
14. Heat exchanger
15. Centrifugal Pump

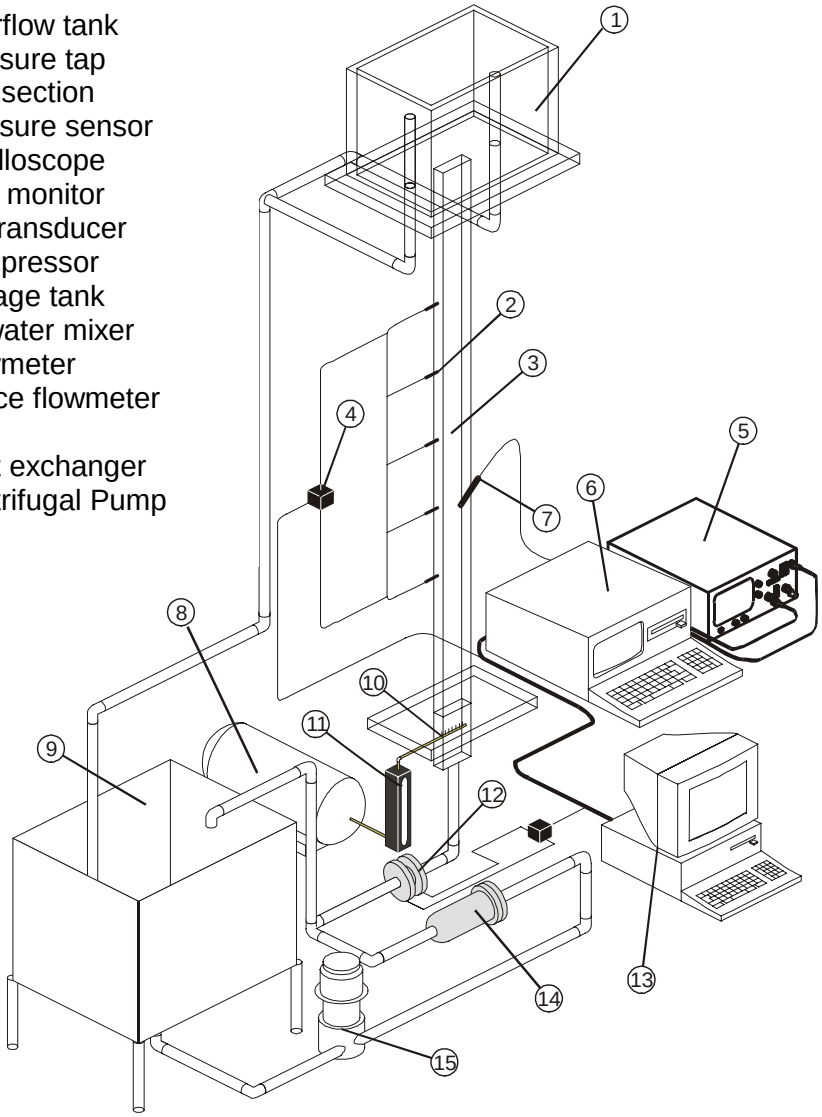

Fig.1 Experimental apparatus

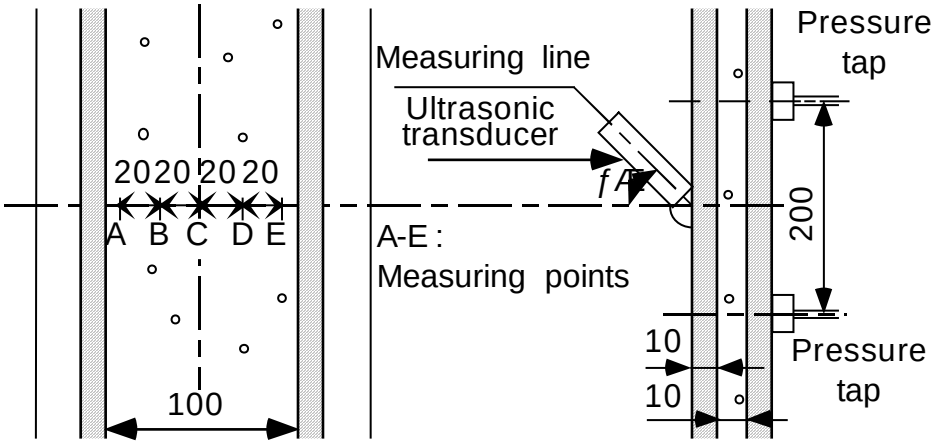

Fig.2 Test section

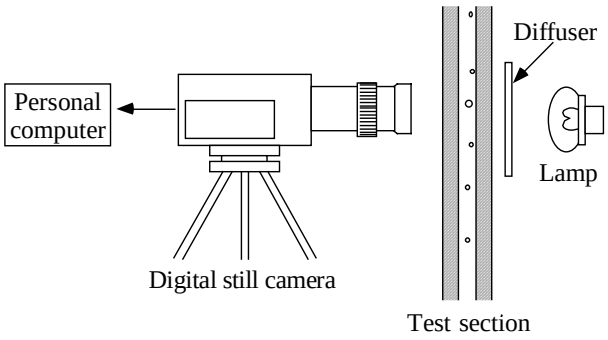

Fig.3 An outline of video camera equipment

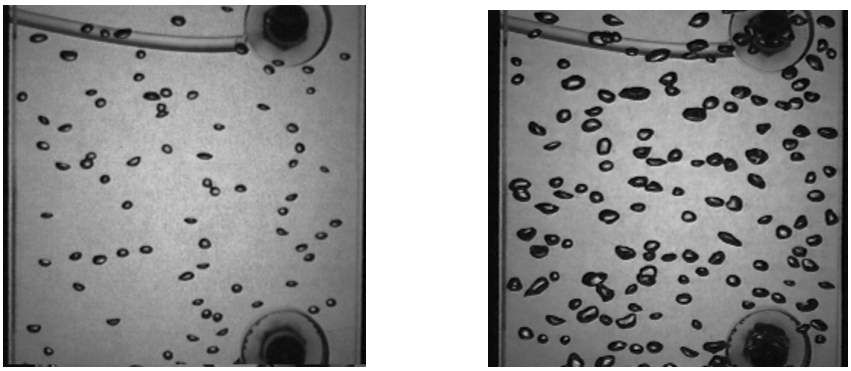

(a) J_L=-0.06m/s,J_G=0.00195m/s, α=1.1%

(b) J_L=-0.12m/s,J_G=0.00418m/s α=5.7%

Fig.4 Typical pictures taken with a video camera

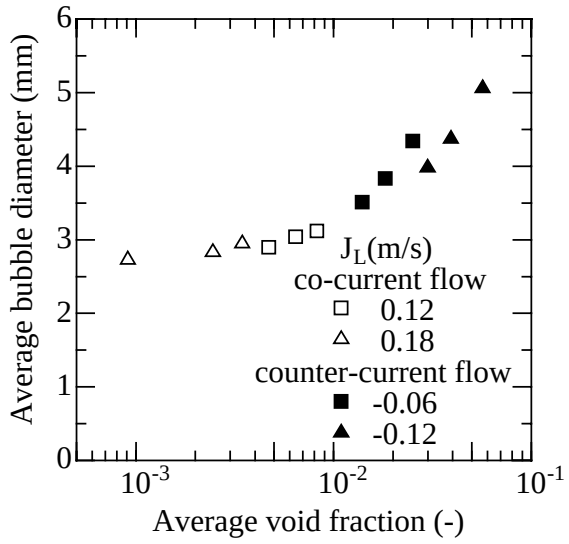

Fig.5 Void fraction and average bubble diameter

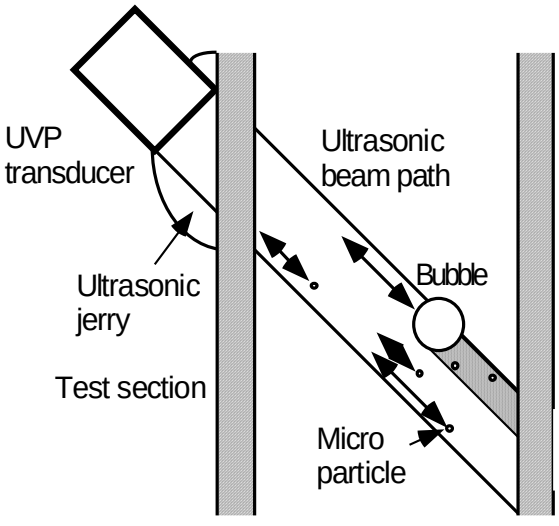

Fig. 6 Blind zone behind bubbles

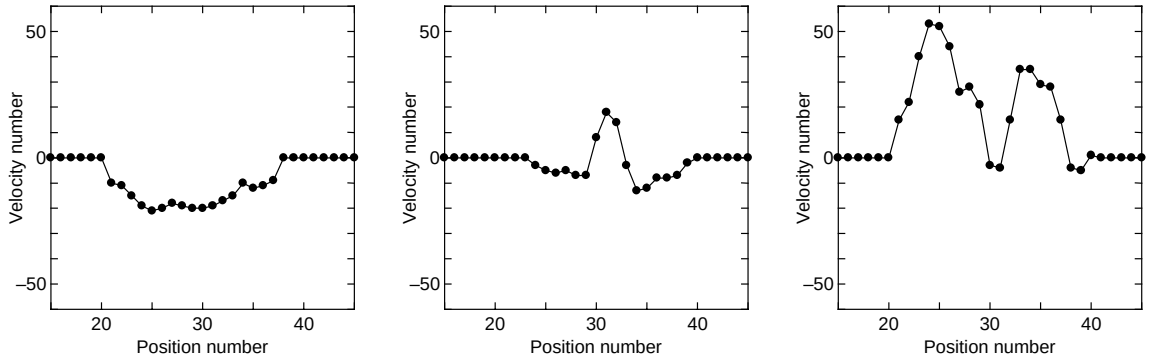

(a) Without bubbles (b) With single bubble (c) Multiple reflection

Fig.7 Typical patterns of velocity profiles

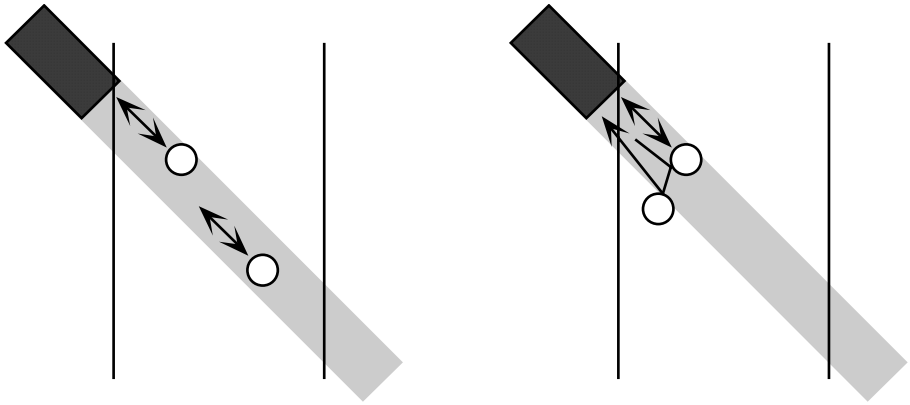

(a) Without multiple-reflection (b) With multiple-reflection

Fig.8 Multiple reflection pattern

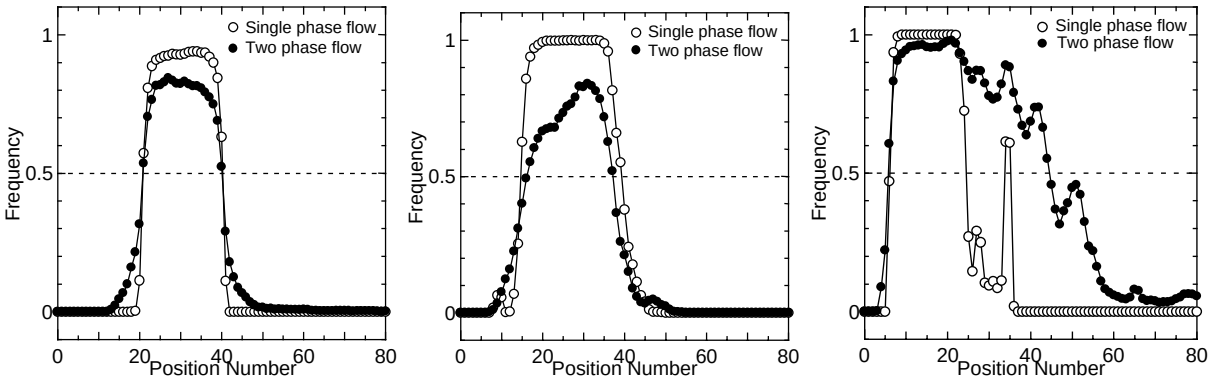

(a) θ = 45ß (b) θ =60ß (c) θ =75ß

Fig.9 Definition of the wall position

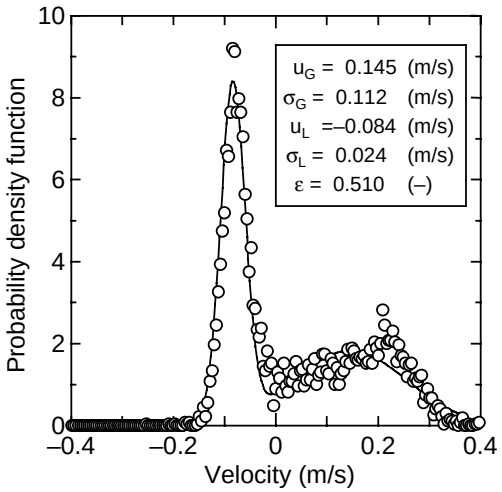

Fig.10 Comparison of the analytical probability density function with the measured one

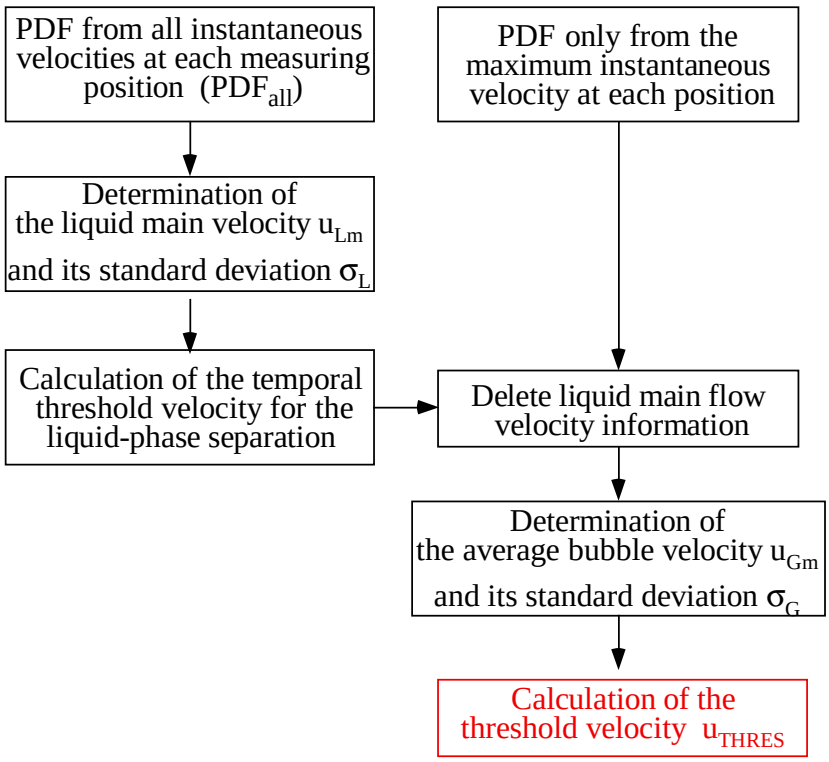

Fig.11 A flow chart of data processing

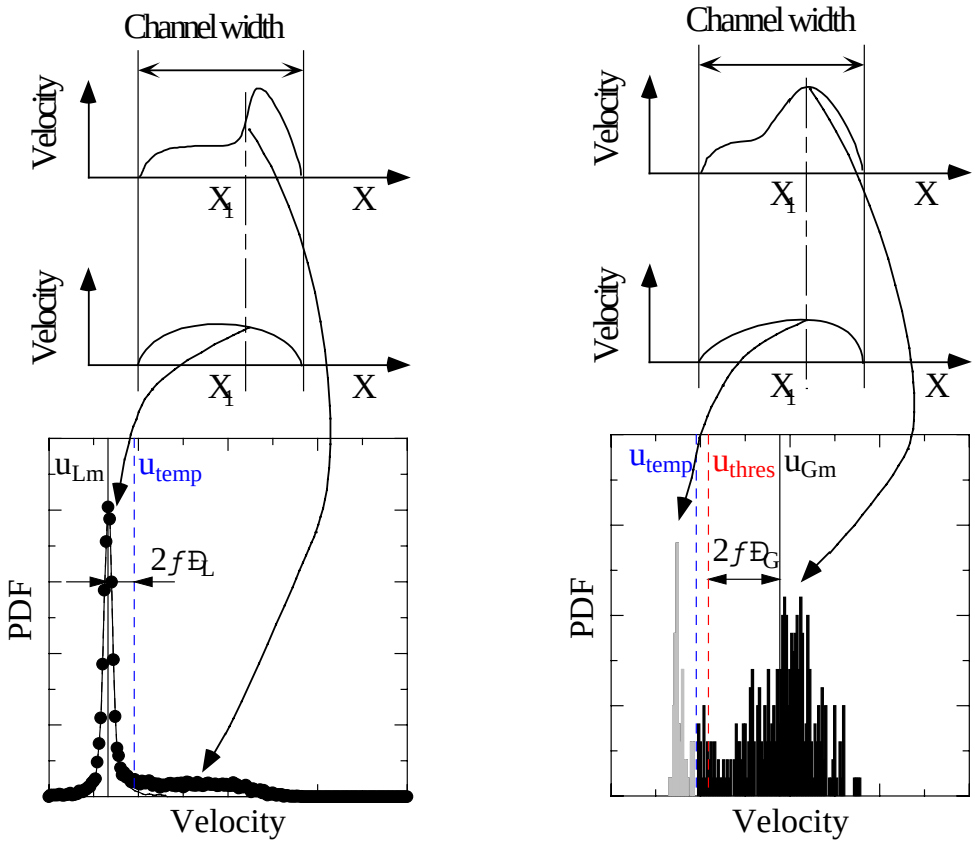

(a)Obtain PDF using all velocity at each measuring point

(b) Obtain PDF using maximum velocity in the channel

Fig. 12 Data processing of phase discrimination

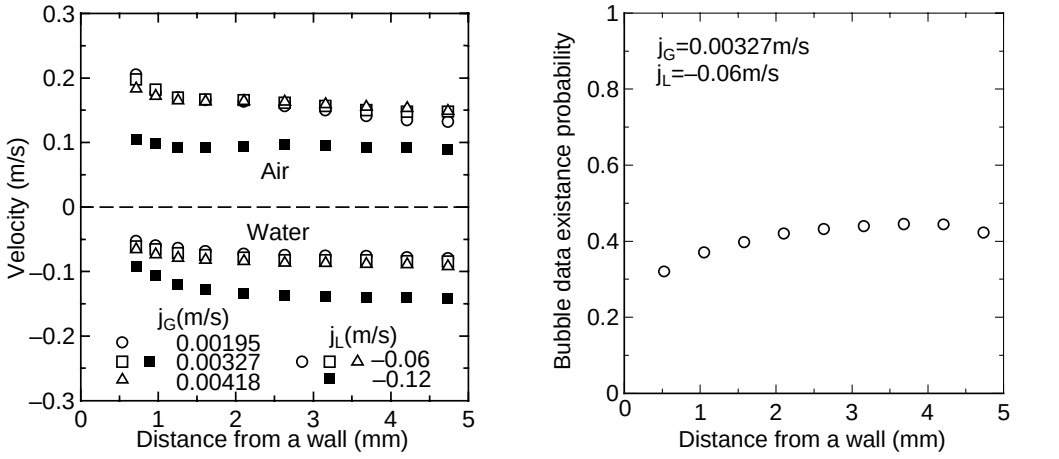

(a) Velocities of both phases

(b) Bubble data existence probability

Fig.13 Typical measured profiles of mixture velocities and bubble data existence probability

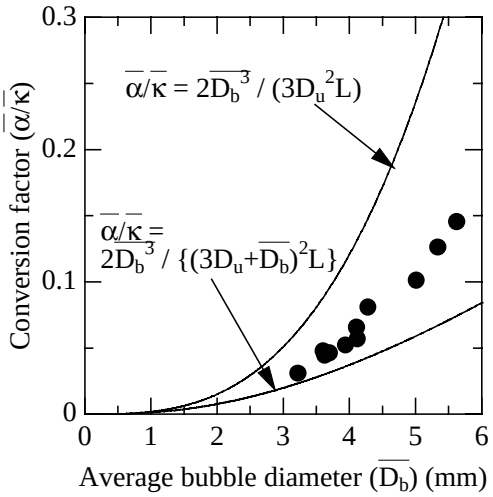

Fig.14 The conversion factor from bubble data existence probability to void fraction

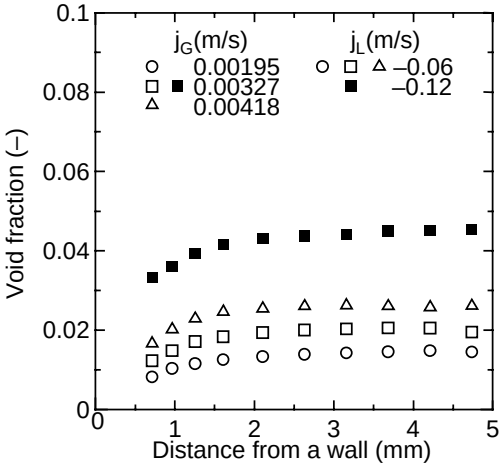

Fig.15 Typical profiles of void fraction

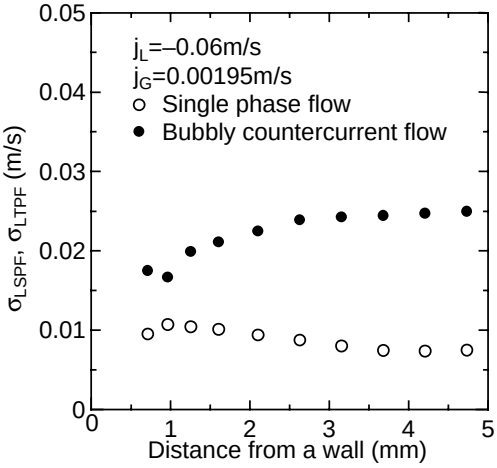

Fig.16 Typical standard deviation profiles of velocity fluctuation

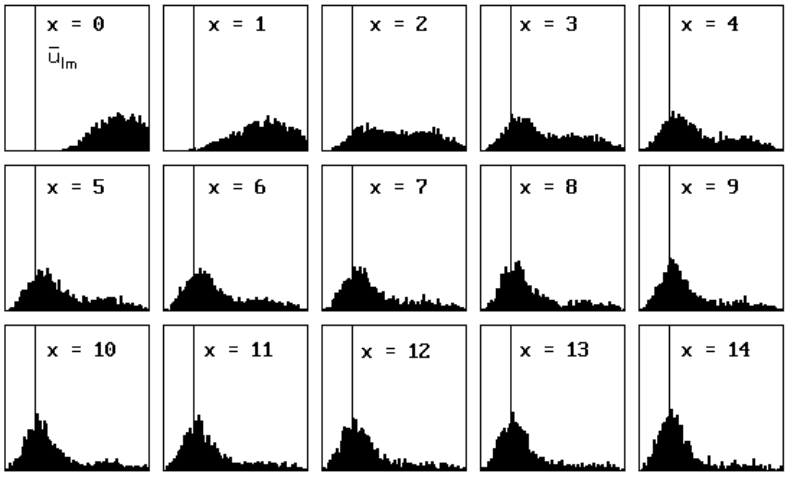

Fig.17 Typical profiles of the probability density function around a bubble

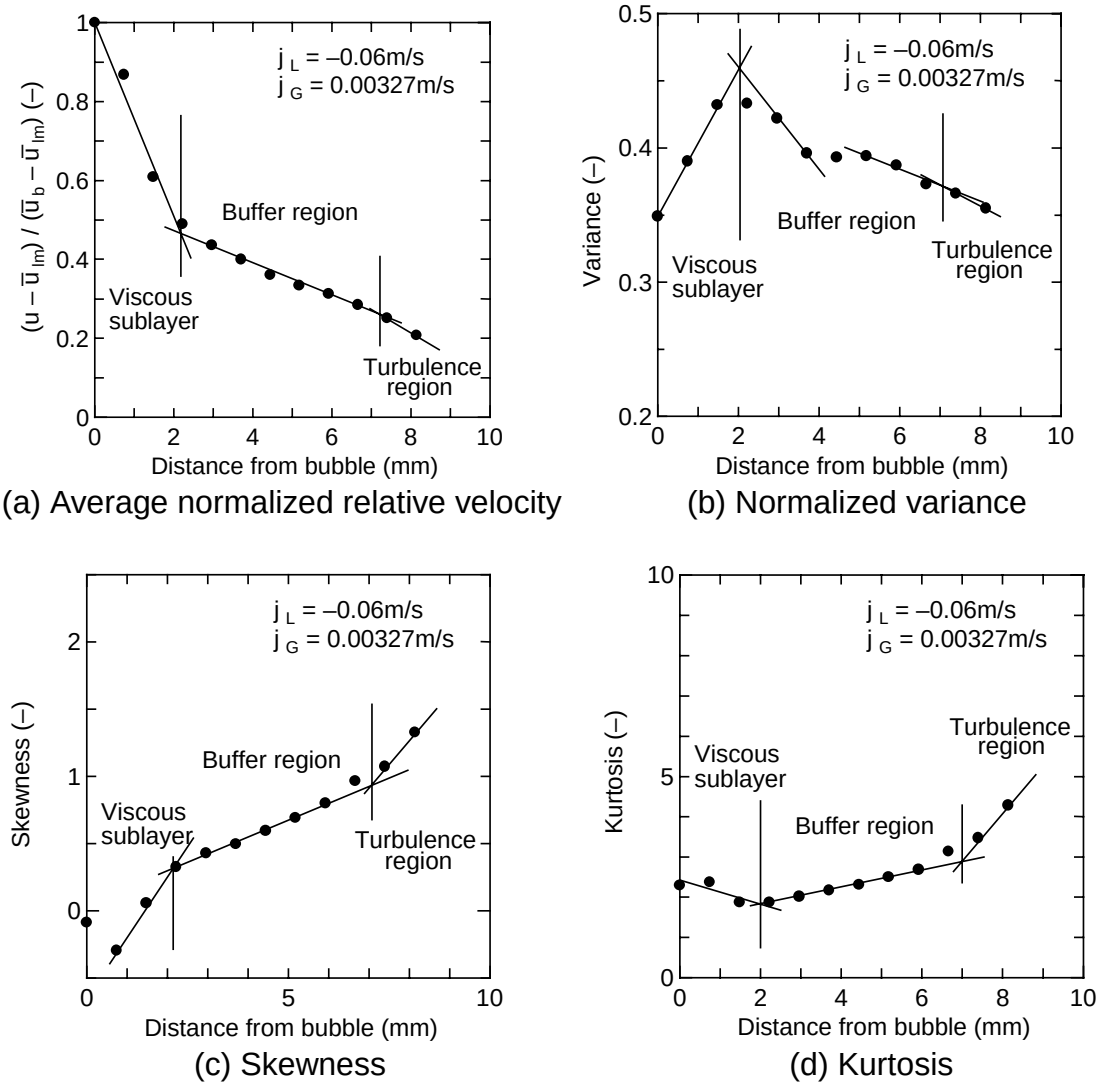

Fig.18 Typical profiles of statistical moments of liquid velocity surrounding bubbles

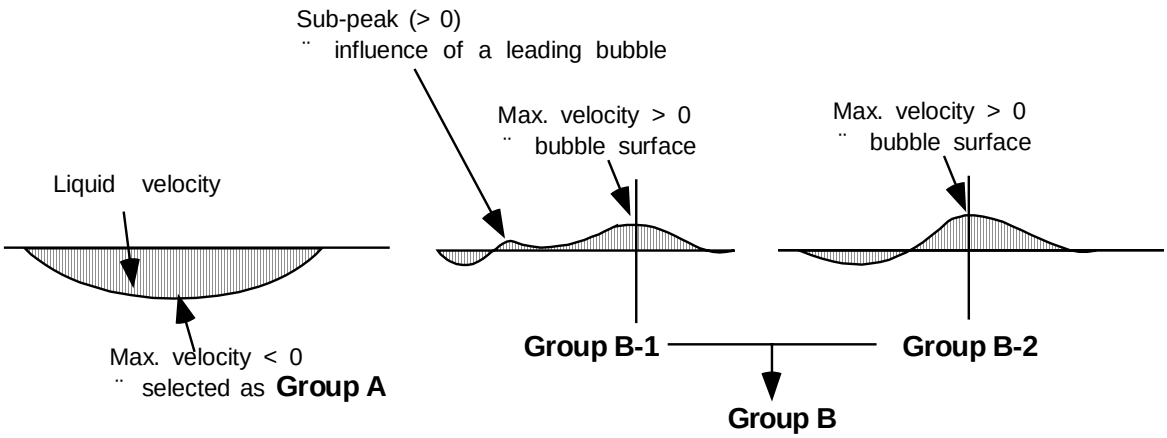

Fig.19 Typical data patterns and their classification

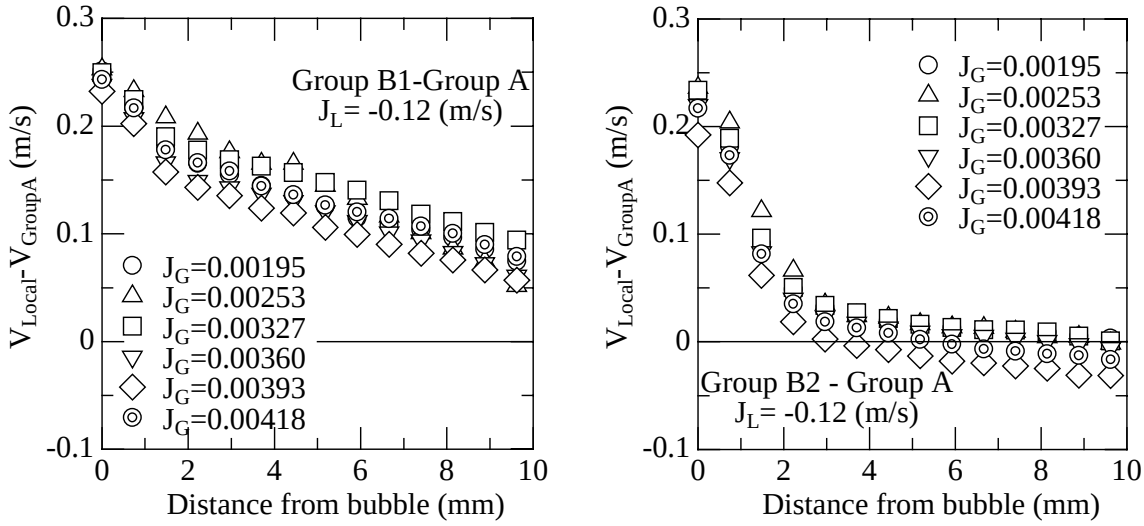

(a)With effect of another bubble wake (Group B1)

(b) Without effect of another bubble wake (Group B2)

Fig.20 Typical average normalized relative velocity surrounding bubbles